Resummed one–loop determination of the phase boundary of the $SU(3)_R \times SU(3)_L$ linear sigma model in the $(m_\pi - m_K)$–plane

T. Herpay*

Department of Physics of Complex Systems, Eötvös University, H-1117 Budapest, Hungary

Zs. Szép†

Research Institute for Solid State Physics and Optics of the Hungarian Academy of Sciences, H-1525 Budapest, Hungary

Complete one-loop parametrization of the linear sigma model is performed and the phase boundary between first order and crossover transition regions of the $m_\pi - m_K$–plane is determined using the optimized perturbation theory as a resummation tool of perturbative series. Away from the physical point the parameters of the model were determined by making use of chiral perturbation theory. Along the diagonal $m_\pi = m_K$ of the mass–plane we estimate $m_\pi^c = 110 \pm 20$ MeV. The location of the tricritical point on the $m_\pi = 0$ axis is estimated in the interval $m_K^{TCP} \in (1700, 1850)$ MeV.

PACS numbers: 11.10.Wx, 11.30.Rd, 12.39.Fe

I. INTRODUCTION

In an attempt to understand the restoration of chiral and axial $U(1)$ symmetries, chiral effective models are actively investigated (see e.g. [1, 2, 3] for some recent works). Effective models indicate a very rich structure for the strongly interacting matter as function of quark masses and various chemical potentials [4, 5]. The effective treatment represents a complementary approach to the lattice QCD field theory which, however based on first principles, has difficulties mainly related to the computational power, in going towards the chiral limit $m_u = m_d = m_s = 0$. These effective models are constructed to share the same global symmetries as the massless QCD. It is expected that the lower m_u, m_d, m_s quark masses are (or alternatively m_π and m_K) the better they work. Universal arguments [6] predict a first order phase transition for the chiral limit. Lattice simulations with staggered quarks with a pion to rho mass ratio tuned to its physical value demonstrate a crossover type transition [7].

In QCD the critical line separating first order transitions from the crossover region in the $m_{u,d} - m_s$–plane is not precisely mapped, because of the difficulties of simulating dynamical fermions. There are several lattice studies with degenerate quarks $m_u = m_d = m_s$, which show that the value of the pion mass on the boundary between the crossover and first order phase transitions drops substantially when finer lattices and improved actions are used, from the initial estimates of $m_\pi^c \approx 290$ MeV [8] or $m_\pi^c \approx 270$ MeV [9] to $m_\pi^c = 67(18)$ MeV [10]. In view of such low values one hopes that the boundary of the phase transition can be investigated reliably using effective chiral models.

Although in principle it is simpler to solve an effective model than QCD, an exact solution cannot be given. Finding a good parametrization and an adequate method of approximation are the key issues when dealing with them. Attempts to parametrize physically the linear sigma model ($L\sigma M$) date back to the early 70's when in a series of papers Haymaker and collaborators have performed it at tree-level and started to calculate one-loop corrections at zero temperature (see [11] and references therein). Recently other parametrizations were proposed in the literature [12, 13] (see also [14]). It turned out that at tree-level it is not possible to fix the parametrization of the model using only the well-known pseudoscalar masses, information is also needed from the less known scalar sector. Moreover, the consequence of performing a tree-level parametrization is that one omits the effect of zero temperature vacuum fluctuations, which logarithmically depend on the renormalization scale. At finite temperature in the broken symmetry phase, the omitted terms have an additional implicit dependence on the temperature through the masses which depends on the order parameter. If the effective model is solved in an approximation which is not renormalization scale invariant, then the renormalization scale appears as any other parameter of the theory, and it has to be included in the process of parametrization in which some quantities calculated at quantum level are matched against their experimentally measured physical values. The effect of the renormalization scale turns out to be both quantitatively and qualitatively important. It can have an effect on the pole structure of the scalar Green's function in the complex plane, as it happened in Ref. [15]. It influences the temperature dependence of the vacuum expectation value, and it can happen that above some temperature there is no solution to the equation of state (see e. g. [16]). The renormalization scale can even change the order of the phase transition. All this reflects the approximate nature of the solution. A good idea is to choose a range of the renormalization scale where its variation affects the other parameters of the theory and the physical quantities less (e.g. trying to achieve approximate renormalization scale independence).

Due to the effects of the renormalization scale mentioned above, it seems customary in the literature not to use the zero temperature quantum fluctuations of the field theory, and forgetting the renormalization issue just solve the model

---

*Electronic address: herpay@complex.elte.hu
†Electronic address: szepzs@achilles.elte.hu

in a statistical mechanics inspired finite temperature quasi-particle approximation. Attempts to renormalize the model in the Hartree approximation of the CJT-formalism [17] were reported in [18], but the result was not satisfactory. Recently much effort has been put in the renormalization of self-consistent resummation schemes of finite temperature QFT [19, 20, 21, 22]. In view of these results, solving the model in a properly renormalized approximation is nowadays a compelling requirement. In the present paper we want to go beyond the tree-level treatment of the model and its quasi-particle thermodynamics as it was treated in [14], and investigate the challenges of solving the renormalized version of the model by taking into account the logarithmic corrections. In particular, we want to investigate the extent they influence the location of the phase boundary in the pion–kaon mass–plane.

In section II we present the one-loop parametrization of the model in the $m_\pi - m_K$–plane. It turns out to be rather hard to find a unique parametrization which works in the relevant region. The thermodynamics and the influence of the logarithmic terms are discussed at the physical point in section III. In section IV we describe our results on the phase boundary, and we conclude in section V.

II. PARAMETRIZATION OF THE MODEL AT ONE-LOOP LEVEL

The Lagrangian of the $SU_L(3) \times SU_R(3)$ symmetric linear sigma model with explicit symmetry breaking terms is given by

$$L(M) = \frac{1}{2}\text{Tr}\left(\partial_\mu M^\dagger \partial^\mu M + \mu^2 M^\dagger M\right) - f_1\left(\text{Tr}\left(M^\dagger M\right)\right)^2 - f_2\text{Tr}\left(M^\dagger M\right)^2 - g\left(\det(M) + \det(M^\dagger)\right) + \epsilon_x \sigma_x + \epsilon_y \sigma_y, \quad (1)$$

where the mixing sector is written in the non-strange (x)- strange (y) basis instead of the original $0-8$ basis, by performing an orthogonal transformation on the fields as in [14] (see Appendix A). The complex 3×3 matrix M defined by the scalar (σ) and pseudoscalar (π) fields can be written as

$$M = \frac{1}{\sqrt{2}}\sum_{i=1}^{7}(\sigma_i + i\pi_i)\lambda_i + \frac{1}{\sqrt{2}}\text{diag}(\sigma_x + i\pi_x, \sigma_x + i\pi_x, \sqrt{2}(\sigma_y + i\pi_y)), \quad (2)$$

where $\lambda_i : \; i = 1\ldots7$ are the Gell-Mann matrices. Isospin breaking is not considered, therefore in the broken phase only the scalar fields σ_x and σ_y have non-zero expectation values: $x := \langle\sigma_x\rangle$, $y := \langle\sigma_y\rangle$. After shifting the fields in the Lagrangian by their expectation values with a little bit of algebra one can perform the traces. Details can be found in [11, 13]. Requiring that the sum of terms linear in the fluctuations vanishes we obtain two equations of state. They are given explicitly in section III. The coefficients of the quadratic terms are the tree-level masses (see Tab. I), while the third and fourth order terms give the three- and four-point interaction vertices.

In what follows, a set of non-linear one-loop equations will be given which determines at $T = 0$ the 8 parameters of the Lagrangian: the couplings μ, f_1, f_2, g, the condensates x, y and the external fields ϵ_x, ϵ_y. Many ways of selecting these equations can be envisaged, see [11] for alternatives. We have chosen to use as input the low lying pseudoscalar mass spectrum, namely the pion, kaon and eta meson masses and the decay constants of the pion and kaon, because they are the best known theoretically.

In the broken phase a resummation is need/home/szepzs/fermion/renorm/kor3/proof/DS9047-1.psed, in order to avoid the appearance of negative mass squares in the finite temperature calculations of one-loop quantities. This can be done for instance using the Optimized Perturbation Theory (OPT) of Chiku and Hatsuda [16]. In the OPT the mass parameter $-\mu^2$ of the Lagrangian, which in the broken phase could be negative, is replaced with an effective (temperature-dependent) mass parameter m^2 which is determined using the criterion of fastest apparent convergence (FAC). The mass term of the Lagrangian reads:

$$L_{mass} = \frac{1}{2}m^2\text{Tr}\,M^\dagger M - \frac{1}{2}(\mu^2 + m^2)\text{Tr}\,M^\dagger M \equiv \frac{1}{2}m^2\text{Tr}\,M^\dagger M - \frac{1}{2}\Delta m^2\text{Tr}\,M^\dagger M, \quad (3)$$

where the finite counterterm Δm^2 is taken into account first at one-loop level.

This resummation method replaces $-\mu^2$ by the effective mass square m^2 in the tree-level masses (see Tab. I), and preserves all the perturbative relations upon which Goldstone's theorem relies [16]. The renormalization is achieved

$m_\pi^2 \;\; = m^2 + 2(2f_1 + f_2)x^2 + 4f_1y^2 + 2gy$	$m_{a_0}^2 \;\; = m^2 + 2(2f_1 + 3f_2)x^2 + 4f_1y^2 - 2gy$
$m_K^2 \;\; = m^2 + 2(2f_1 + f_2)(x^2 + y^2) + 2f_2y^2 - \sqrt{2}x(2f_2y - g)$	$m_\kappa^2 \;\; = m^2 + 2(2f_1 + f_2)(x^2 + y^2) + 2f_2y^2 + \sqrt{2}x(2f_2y - g)$
$m_{\eta_{xx}}^2 = m^2 + 2(2f_1 + f_2)x^2 + 4f_1y^2 - 2gy$	$m_{\sigma_{xx}}^2 = m^2 + 6(2f_1 + f_2)x^2 + 4f_1y^2 + 2gy$
$m_{\eta_{yy}}^2 = m^2 + 4f_1x^2 + 4(f_1 + f_2)y^2$	$m_{\sigma_{yy}}^2 = m^2 + 4f_1x^2 + 12(f_1 + f_2)y^2$
$m_{\eta_{xy}}^2 = -2gx$	$m_{\sigma_{xy}}^2 = 8f_1xy + 2gx$

TABLE I: The squared masses of the (pseudo)scalar nonet appear in the (first) second column. The last three rows represent the mixing sectors. They can be written in the conventional basis using the formulas of Appendix A.

both in the symmetric and the broken phase by the following counterterms

$$\delta\mu^2 = \frac{(5f_1 + 3f_2)\Lambda^2}{\pi^2} - \frac{(5f_1 + 3f_2)m^2 - g^2}{\pi^2} \ln\frac{\Lambda^2}{l^2}, \tag{4}$$

$$\delta g = \frac{3g(f_1 - f_2)}{2\pi^2} \ln\frac{\Lambda^2}{l^2}, \tag{5}$$

$$\delta f_1 = \frac{13f_1^2 + 12f_1 f_2 + 3f_2^2}{2\pi^2} \ln\frac{\Lambda^2}{l^2}, \tag{6}$$

$$\delta f_2 = \frac{3f_1 f_2 + 3f_2^2}{\pi^2} \ln\frac{\Lambda^2}{l^2}, \tag{7}$$

where Λ is the 3d regularization cutoff, and l is the renormalization scale. Note that only the mass counterterm differs from its standard expression [11]. In the present form this counterterm is temperature-dependent through the effective mass, but this temperature dependence is canceled by higher-loop terms [16, 23]. In what follows, all quantities and equations are renormalized without any change in the notations.

The above mentioned FAC criterion, which determines the effective mass square m^2, is realized in the present case by the requirement that the pole and the residue of the one-loop pion propagator

$$D_\pi(p) = \frac{iZ_\pi^{-1}}{p^2 - m_\pi^2 - \Sigma_\pi(p^2, m_i, l)}, \tag{8}$$

stay equal to their tree-level values. Here we anticipated that we also need a finite wave function renormalization in order to make the residuum equal to 1, and rescaled the pion fields as $\pi \to Z_\pi^{-\frac{1}{2}}\pi$.

According to this FAC criterion the inverse of the finite wave function renormalization constant is

$$Z_\pi^{-1} := 1 - \left.\frac{\partial\Sigma_\pi(p^2, m_i, l)}{\partial p^2}\right|_{p^2 = M_\pi^2}. \tag{9}$$

The one-loop pion pole mass

$$M_\pi^2 = -\mu^2 + (4f_1 + 2f_2)x^2 + 4f_1 y^2 + 2gy + \mathrm{Re}\left\{\Sigma_\pi(p^2 = M_\pi^2, m_i, l)\right\} \tag{10}$$

has to be equal to its tree-level value ($M_\pi \overset{!}{=} m_\pi$). Therefore, using the expression of the tree-level pion mass of Tab. I, the following "gap" equation can be obtained for the effective mass:

$$m^2 = -\mu^2 + \mathrm{Re}\left\{\Sigma_\pi(p^2 = m_\pi^2, m_i(m^2), l)\right\}, \tag{11}$$

where the m^2-dependence of the self-energy (through the tree-level masses) is explicitly shown. The different contributions to the self-energy are depicted in Fig. 1.

The effective mass can be replaced by the pion mass by expressing it from its tree-level formula. Then (11) can be interpreted as a zero temperature gap-equation for the pion mass:

$$m_\pi^2 = -\mu^2 + (4f_1 + 2f_2)x^2 + 4f_1 y^2 + 2gy + \mathrm{Re}\left\{\Sigma_\pi(p^2 = m_\pi^2, m_i(m_\pi), l)\right\}, \tag{12}$$

where the tree masses of all mesons are expressed through the pion mass. A similar gap-equation will be used in the thermodynamical calculations for the temperature dependence of the pion mass. At $T = 0$, the task is "reversed": the pion mass is known and (12) belongs to the set of equations, which determines the parameters. We have chosen to express the effective mass m^2 from the tree-level mass formula of the pion because the pion has the smallest mass, and positive solutions of (12) ensure the positiveness of all the other masses. We use the kaon and eta masses, the relations of the Partially Conserved Axial-Vector Current (PCAC) for the pion and kaon at one-loop order, and the two equations of state to fix the remaining parameters.

The one-loop kaon propagator is the following:

$$D_K(p) = \frac{iZ_K^{-1}}{p^2 - m_K^2 - \Sigma_K(p^2, m_i, l)}. \tag{13}$$

Z_K^{-1} and the one-loop pole mass of the kaon M_K can be calculated similarly as in the case of the pion:

$$Z_K^{-1} := 1 - \left.\frac{\partial\Sigma_K(p^2, m_i, l)}{\partial p^2}\right|_{p^2 = M_K^2}, \tag{14}$$

and

$$M_K^2 = -\mu^2 + 2(2f_1 + f_2)(x^2 + y^2) + 2f_2 y^2 - \sqrt{2}x(2f_2 y - g) + \mathrm{Re}\left\{\Sigma_K(p^2 = M_K^2, m_i, l)\right\}. \tag{15}$$

FIG. 1: The physical content of the one-loop pseudoscalar self-energies.

The description of the η and η' mesons is slightly more complicated because of the mixing in the $x-y$ sector ($0-8$ in the conventional basis). The propagator is a 2×2 matrix, and pole masses are defined as the real part of the solutions of the following equations

$$\text{Det} \left. \begin{pmatrix} p^2 - m^2_{\eta_{xx}} - \Sigma_{\eta_{xx}}(p^2, m_i, l) & -m^2_{\eta_{xy}} - \Sigma_{\eta_{xy}}(p^2, m_i, l) \\ -m^2_{\eta_{xy}} - \Sigma_{\eta_{xy}}(p^2, m_i, l) & p^2 - m^2_{\eta_{yy}} - \Sigma_{\eta_{yy}}(p^2, m_i, l) \end{pmatrix} \right|_{p^2 = M^2_\eta, M_{\eta'}} = 0. \tag{16}$$

This yields two equations for the mass eigenvalues M_η, $M_{\eta'}$:

$$M^2_\eta = \frac{1}{2}\text{Re}\left\{ m^2_{\eta_{xx}} + \Sigma_{\eta_{xx}}(p^2 = M^2_\eta, m_i, l) + m^2_{\eta_{yy}} + \Sigma_{\eta_{yy}}(p^2 = M^2_\eta, m_i, l) \right.$$
$$\left. - \sqrt{(m^2_{\eta_{xx}} + \Sigma_{\eta_{xx}}(p^2 = M^2_\eta, m_i, l) - m^2_{\eta_{yy}} - \Sigma_{\eta_{yy}}(p^2 = M^2_\eta, m_i, l))^2 + 4(m^2_{\eta_{xy}} + \Sigma_{\eta_{xy}}(p^2 = M^2_\eta, m_i, l))^2} \right\}, \tag{17}$$
$$M^2_{\eta'} = \frac{1}{2}\text{Re}\left\{ m^2_{\eta_{xx}} + \Sigma_{\eta_{xx}}(p^2 = M^2_{\eta'}, m_i, l) + m^2_{\eta_{yy}} + \Sigma_{\eta_{yy}}(p^2 = M^2_{\eta'}, m_i, l) \right.$$
$$\left. + \sqrt{(m^2_{\eta_{xx}} + \Sigma_{\eta_{xx}}(p^2 = M^2_{\eta'}, m_i, l) - m^2_{\eta_{yy}} - \Sigma_{\eta_{yy}}(p^2 = M^2_{\eta'}, m_i, l))^2 + 4(m^2_{\eta_{xy}} + \Sigma_{\eta_{xy}}(p^2 = M^2_{\eta'}, m_i, l))^2} \right\} \tag{18}$$

The definitions (10), (15), (17) and (18) of the pole masses give the correct one-loop masses only when the self-energy is not complex. We note that if the tree-level masses are close to their experimental values, then by looking at the self-energy contributions of pion and kaon in Fig. 1, one can recognize that they have no imaginary part for $p^2 = m^2_\pi$ and $p^2 = m^2_K$, respectively. This is also true in the case of the η self-energy. It turns out that the η' self-energy has an imaginary part at the pole-mass determined as the zero of the real part of the self-energy except the narrow range of 1820 MeV $< l <$ 1880 MeV. For this reason we decided not to include the one-loop equation for $M_{\eta'}$ into the set of equations used for the parametrization. We make up for the missing equation by extending FAC criterion to the one-loop kaon mass too. This condition reads:

$$M^2_K \overset{!}{=} m^2_K = m^2_\pi - 2gy + 4f_2 y^2 - \sqrt{2}x(2f_2 y - g). \tag{19}$$

Two more equations are provided by the one-loop PCAC relations which according to [11] reads as

$$f_\pi = Z_\pi^{-\frac{1}{2}} \frac{-iD_\pi^{-1}(p=0)}{M^2_\pi} x, \tag{20}$$

$$f_K = Z_K^{-\frac{1}{2}} \frac{-iD_K^{-1}(p=0)}{M^2_K} \frac{x + \sqrt{2}y}{2}. \tag{21}$$

As shown in Appendix C, these equations can be rewritten in an explicitly renormalization scale-independent form.
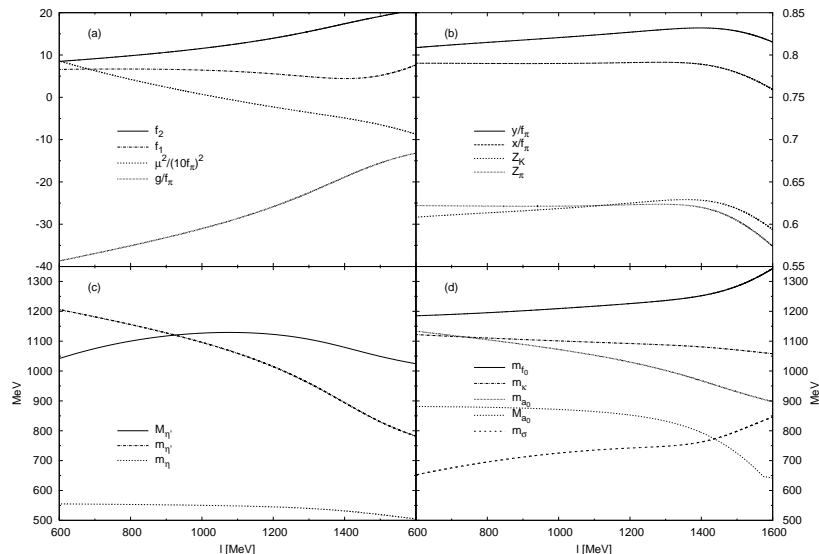
FIG. 2: The renormalization scale dependence of various quantities at the physical point: the parameters (a), the non-strange (x) and strange (y) vacuum expectation values and the finite wave function renormalization constants Z_π and Z_K (b), the pseudoscalar masses (c), and the scalar masses (d).

Finally, the last two parameters, the two symmetry breaking external fields ϵ_x and ϵ_y are determined by the one-loop equations of state, with the help of zero temperature chiral Ward identities (Appendix B):

$$\epsilon_x = Z_\pi^{-1}\left(-iD_\pi^{-1}(p=0)\right)x, \tag{22}$$

$$\epsilon_y = Z_K^{-1}\left(-iD_K^{-1}(p=0)\right)\left(\frac{x}{\sqrt{2}}+y\right) - Z_\pi^{-1}\left(-iD_\pi^{-1}(p=0)\right)\frac{x}{\sqrt{2}}. \tag{23}$$

One can notice that, since OPT preserves Ward identities at tree and at one-loop level as well, the above parametrization, in which the tree-level masses of pion and kaon equal the one-loop masses, ensures at zero temperature the validity of Goldstone's theorem for both pion and kaon.

A. Parametrization at the physical point

The parameters were determined as follows. From (10) and (19) one can express μ^2 and g, respectively. Next, from the system of 4 non-linear equation (15), (17), (20), (21) one can numerically determine f_1, f_2, x, and y as functions of the renormalization scale l. Going back to (10) and (19) one can compute μ^2 and g, respectively. Substituting these parameters into (22) and (23) one can determine ϵ_x and ϵ_y. Unlike the tree-level parametrization case [14], now all scalar masses are predicted.

The numerical solution for different renormalization scales l is presented in Fig. 2 (a) for the physical point, where $m_\pi = 138$ MeV, $m_K = 495.6$ MeV, $m_\eta = 547.8$ MeV, $f_\pi = 93$ MeV, and $f_K = 113$ MeV. In figure Fig. 2 (b) one can see the renormalization scale (l) dependence of the non-strange (x) and strange (y) vacuum expectation values and of the finite wave function renormalization constants Z_π and Z_K. They have a plateau for $l < 1400$ MeV, and the tree-level $m_{\eta'}$ (see Fig. 2 (c)) is the closest to its physical value in the region $l \in (1000, 1400)$ MeV, where the variation of the tree-level scalar masses (see Fig. 2 (d)) is the mildest too. We have decided to use in our thermodynamical investigation this range of the renormalization scale in which the tree-level masses entering into the propagators of Fig. 1 are reasonably close to their experimentally measured values. In Fig. 2 (c, d) we present an estimation of the predicted one-loop pole-masses based on the real parts of the corresponding self-energies. This is a good approximation in the case of η', a_0 and f_0 since the zeros of the inverse propagators correlate well with the location of the well-defined peak in the corresponding spectral functions. The one-loop mass M_{f_0}, which is not shown in the figure, has a rather large value in the present range of the renormalization scale (decreasing from $M_{f_0} = 2000$ MeV for $l = 1000$ MeV to $M_{f_0} = 1400$ MeV for $l = 1400$ MeV). The shapes of the spectral functions of κ and σ (see Fig. 2 for ρ_σ) are more complicated, they have a threshold dominated peak with large width, and are very sensitive to the renormalization scale. In this case, it would be more appropriate to define the mass and width of a decaying particle as the real and imaginary part of a complex pole. In the $O(N)$ model in the large N approximation [24], this continuation into the second Riemann sheet was performed in the sigma channel and the poles of the propagators were determined. In this model the continuation of the propagators into the complex plane would be more difficult due to the appearance of many decay thresholds and is beyond the scope of the present investigation.
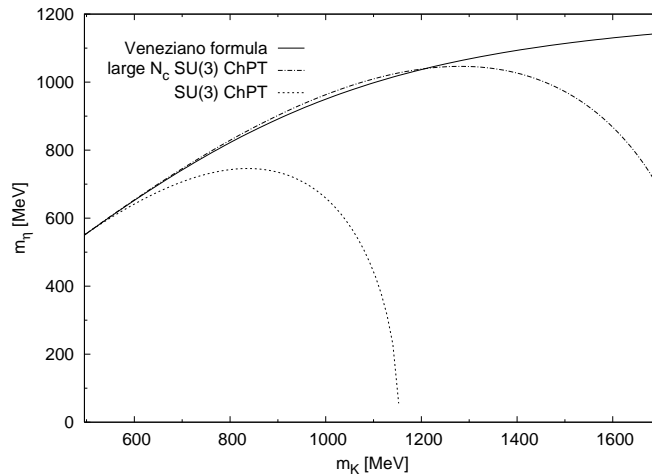
FIG. 3: The kaon mass dependence of m_η as given by ChPT and the Veneziano formula for $m_\pi = 10$ MeV.

B.   Parametrization in the $m_\pi - m_K$–plane

Since we are interested in the phase boundary on the $m_\pi - m_K$-plane, we have to take into account the variation of the parameters with m_π and m_K. A method for the parametrization away from the physical point was proposed in [14], which relies on the formulas provided by the Chiral Perturbation Theory (ChPT) [25]. Because our present parametrization does not use the η' meson, we make use of the $SU(3)$ ChPT describing the chiral dynamics of the pseudoscalar octet. In the large N_c limit, the formulas for the pion, kaon mass dependence of the decay constants and of the η mass up to $\mathcal{O}(1/f^2)$ read as [26]:

$$f_\pi = f\left(1 + 4L_5\frac{m_\pi^2}{f^2}\right), \tag{24}$$

$$f_K = f\left(1 + 4L_5\frac{m_K^2}{f^2}\right), \tag{25}$$

$$m_\eta^2 = \frac{4m_K^2 - m_\pi^2}{3} + \frac{32}{3}(2L_8 - L_5)\frac{\left(m_K^2 - m_\pi^2\right)^2}{f^2}, \tag{26}$$

where L_5 and L_8 are low energy constants and f is the decay constant in the chiral limit. All the parameters of the large N_c limit of the $SU(3)$ ChPT can be determined at the physical point from the equations above. Their values, $L_5 = 2.0152 \cdot 10^{-3}$, $L_8 = 8.472 \cdot 10^{-4}$ and $f = 91.32$ MeV, are fixed for all values of m_π and m_K.

For low values of m_π and m_K the sensitivity to the renormalization scale of the $L\sigma M$ is bigger than the uncertainties coming from the omission of the chiral logarithms. As an effect of these chiral logarithms, for large values of m_K, the formula of the $SU(3)$ ChPT yields a decreasing value for m_η for increasing m_K, see Fig. 3. If we use (26), the same behavior occurs at a larger value, which is around $m_K \approx 1300$ MeV. This is non-physical as both the kaon and the eta particles have to decouple in order to arrive at the O(4) model for $m_K \to \infty$. This shows the failure of the ChPT at high values of the kaon mass.

In view of the bad behavior of m_η determined using large N_c ChPT, we have used, as an alternative, the following mass-formula by Veneziano [27] :

$$m_\eta^2 = m_K^2 + \frac{1}{2}\Delta m_{\eta 0}^2 - \frac{1}{2}\sqrt{\left(2m_K^2 - 2m_\pi^2 - \frac{1}{3}\Delta m_{\eta 0}^2\right)^2 + \frac{8}{9}\Delta m_{\eta 0}^4}. \tag{27}$$

$\Delta m_{\eta 0}^2$ is the non-perturbative gluonic mass contribution in the singlet channel of the mixing $\eta - \eta'$ sector, related to the axial $U(1)$ dynamics. Using the values of the masses at the physical point in (27) one can fix the value of the extra mass contribution: $\Delta m_{\eta 0}^2 = 2.3$ GeV^2. One can see in Fig. 3 that this parametrization gives for m_η values which are almost identical to the values coming from the formula of ChPT in the large N_c limit, up to values of m_K for which ChPT breaks down.

We note, that in the original paper $\Delta m_{\eta 0}^2$ was determined using the trace of the 2×2 matrix of the mixing $\eta - \eta'$ sector. We indulged in modifying the procedure in order to make contact with the ChPT in the large N_c limit, as m_η obtained form (27) with the original parametrization is always smaller than the value given by the large N_c ChPT.

The continuation onto the $m_\pi - m_K$–plane of f_π, f_K, and m_η, based on the formulas of this subsection, allow us to determine the parameters as described in II A in a wide region of the mass-plane, except for high values of m_K, near the $m_\pi = 0$ axis.

III. COMPLETE 1–LOOP THERMODYNAMICS OF THE LσM

With the intention of determining the order of the phase transition in the pion–kaon mass–plane we have to monitor the order parameters as functions of temperature. They are obtained from a set of three equations: two equations of state for x and y and a gap-equation for the pion mass. The temperature dependence of the order parameters at finite T can be obtained from the equations of state:

$$-\epsilon_x + m^2 x + 2gxy + 4f_1 xy^2 + (4f_1 + 2f_2)x^3 + \sum_i J_i t_i^x I(l, m_i(T), T) + \Delta m^2 x = 0, \qquad (28)$$

$$-\epsilon_y + m^2 y + gx^2 + 4f_1 x^2 y + 4(f_1 + f_2)y^3 + \sum_i J_i t_i^y I(l, m_i(T), T) + \Delta m^2 y = 0, \qquad (29)$$

where in the tadpole integral $I(l, m_i(T), T)$ we have explicitly displayed the implicit temperature dependence of the tree-level masses, expressed with the pion mass determined by the gap-equation

$$m_\pi^2 = -\mu^2 + (4f_1 + 2f_2)x^2 + 4f_1 y^2 + 2gy + \Sigma_\pi(p^2 = m_\pi^2, m_i(m_\pi), l) + \Sigma_\pi^T(\omega = 0, m_i(m_\pi)). \qquad (30)$$

The sum goes over all mass eigenstate meson fields with isospin multiplicity factor J_i: $J_{\pi,a_0} = 3$, $J_{K,\kappa} = 4$, and $J_{\eta,\eta',\sigma,f_0} = 1$. The coefficients t_i^x and t_i^y appearing in (28) and (29) are listed in Appendix C of [14]. The standard one-loop integrals appearing in the formulas above can be found for instance in [16]. In the present study we use the one-loop bubble integrals appearing in (30) for $|\mathbf{p}| = 0$, corresponding to particles at rest. As in zero temperature case, at finite temperature OPT guarantees through the gap-equation the validity of Goldstone's theorem for the pion. Following Ref. [16], Σ_π^T, the finite-temperature part of the self-energy, is taken not on the mass-shell, but instead at $\omega = 0$. This is done because above a given temperature $\Sigma_\pi(T)(\omega = m_\pi(T), \mathbf{0})$ becomes complex, and the real solution of the gap equation ceases to exist. At the physical mass-point this temperature is typically below the value of the pseudocritical temperature, invalidating the study of the phase transition. The imaginary part is produced by one-loop bubble integrals where two unequal masses m_1 and m_2 appear, when the relation $\omega = m_\pi < |m_1 - m_2|$ is satisfied. It has the consequence that we can not regard the pion gap-equation as the equation determining the "true" one-loop mass of the pion. Due to the imaginary part of the self-energy the most adequate way of determining the pion mass would be to look for a complex pole of the pion propagator. Still, in the present work we content ourselves with the study of the spectral function of the pion, which, as we will see, in certain temperature ranges also provides information on the pion mass.

A. Influence of the logarithmic terms

In order to estimate the influence of the logarithmic terms on the solution of the equations of state we have performed the following check. We have taken the parameters determined with the one-loop parametrization presented in Sec. II, and modified the value of μ^2 such as to incorporate the zero temperature logarithmic terms. Then, at finite temperature, we have solved the gap equation and the two equations of state without taking into account the logarithmic terms, which implicitly depend on the temperature through the masses. The difference between these expectation values and the ones calculated with the logarithmic terms (and with the original, unmodified value of μ^2) is only due to the temperature dependence of the logarithmic terms. This can be seen in Fig. 4: without the logarithmic terms the pseudocritical temperature is lower by about 20%. The variation of strange condensate with the temperature is significantly different in the two cases. We notice that at high temperature the solution obtained with logarithmic term included ceases to exist, as was also observed in [16]. This is a non-physical phenomenon, it happens before the restoration of chiral symmetry completes. We consider the solution reliable up to temperature values which are below the turning point in x and y.
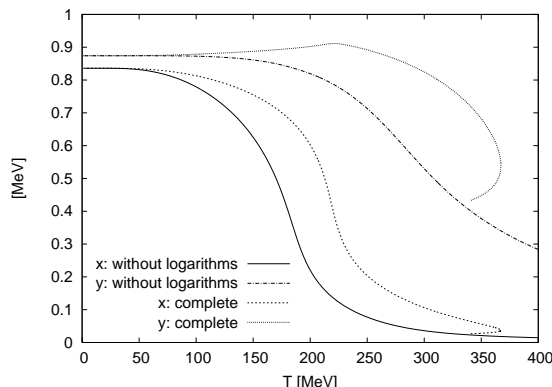
FIG. 4: Comparison of the temperature dependence of strange (y) and non-strange (x) condensates with and without the inclusion of the logarithms for $l = 1200$ MeV.
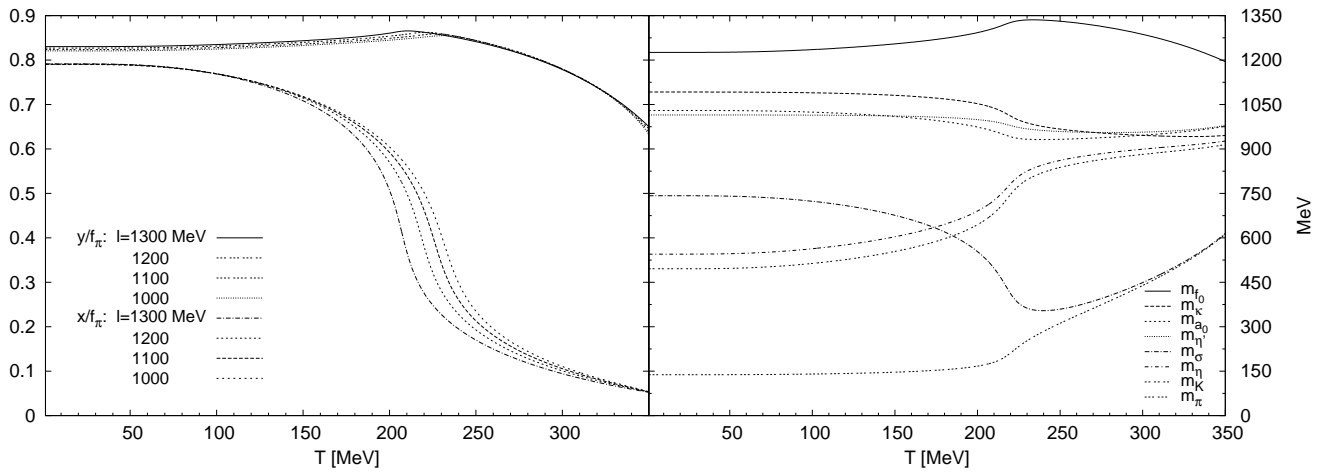
FIG. 5: The temperature dependence of non-strange (x) and strange (y) order parameters for different values of the renormalization scale (l.h.s) and the T-dependence of the tree-level masses for $l = 1200$ MeV (r.h.s).

B. The solution at the physical point

At the physical point and in the investigated range of the renormalization scale, the behavior of the non-strange order parameter shows a smooth restoration of the $SU(2)$ chiral symmetry. The pseudocritical temperature moderately depends on the renormalization scale. The strange order parameter varies less and it is approximately scale-independent until the solution is reliable, see the left panel of Fig. 5. The right panel shows that the tree-level $SU(2)$ mass partners tend towards degeneracy as the temperature increases. Unfortunately the solution falls dead before the restoration of the complete $SU(3)$ symmetry, due to the effect of the logarithmic terms (see III A).

Fig. 6 illustrates the temperature dependence of the spectral functions in the pseudoscalar and scalar channels and the behavior of the zeros of the real part of the inverse pion and sigma propagators. At low temperature the spectral function in the pion channel develops a peak whose location is close to the physical mass value of the pion. Close to the pseudocritical temperature there are significant changes in the peak structure. In this temperature range, based on the spectral function, one can not determine the true pion pole-mass. In this range, the tree-level pion mass, which is the solution of the gap-equation (12) interpolates between various zeros of the inverse propagator, see the left panel of Fig. 6. At high temperature the spectral function has a well defined peak again, whose location correlates with the zero of the inverse pion propagator.

At low temperature the spectral function in the sigma channel has a large width and the zeroes of the real part of the inverse propagator are very sensitive to the renormalization scale, therefore the sigma pole mass can not be estimated. We can define the pole mass only at high temperature, where the spectral function develops a well–defined peak, correlated with the zero of the inverse sigma propagator. Increasing the temperature its location approaches the location of the peak in the pion channel and eventually they become degenerate. This shows that the one-loop masses of the pion and sigma also reflect the restoration of the $SU(2)$ chiral symmetry at high temperature.

FIG. 6: The spectral function of the pion (l.h.s.) and sigma (r.h.s.) for various values of the temperature and $l = 1200$ MeV. The zeros of the real part of the inverse pion/sigma propagators and the corresponding tree-level masses are also depicted, as lines in the $T - \omega$ plane.

IV.   THE PHASE BOUNDARY ON THE $m_\pi - m_K$−PLANE

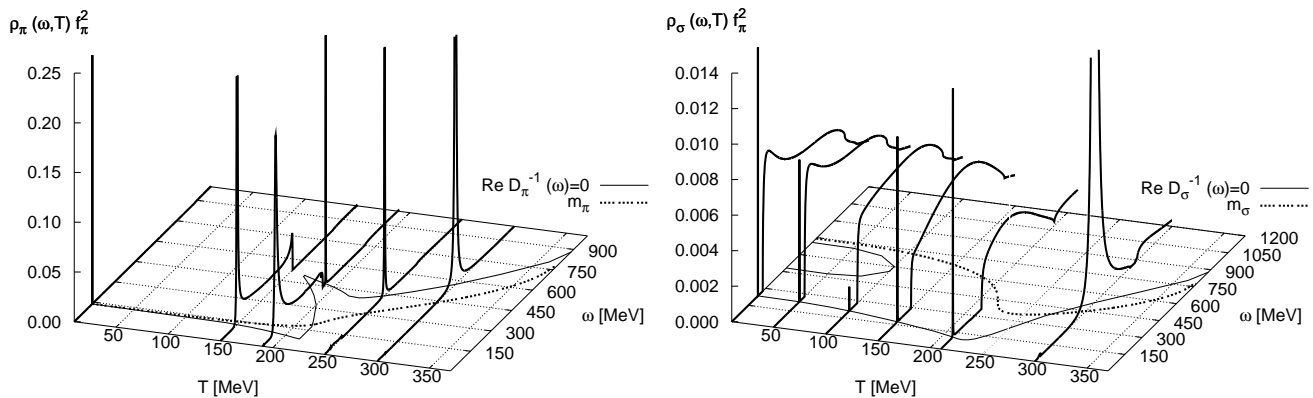The main result of our work is the determination of the boundary between the region where a crossover transition occurs, with a smooth variation of the order parameters, and a first order phase transition region, which is signaled by the multivaluedness of the order parameters.

It is remarkable, that at large values of the kaon mass, the boundary proves to be independent of the renormalization scale [1]. For large values of m_K the existence of a scaling region belonging to a tricritical point (TCP), with mean-field exponent can be confirmed. This is a new feature of the complete QFT treatment, it was not observed using tree-level parametrization! From mean-field studies (see e.g. [28]) it is known that near the TCP the boundary of the edge of the first order region deviates from the $m_{u,d} = 0$ axis of the quark mass-plane according to $m_{u,d} \approx (m_s^{TCP} - m_s)^{5/2}$. Using the tree-level formulas of ChPT, for m_π^2 and m_K^2, namely $m_\pi^2 = 2\hat{m}B_0$, $m_K^2 = (\hat{m} + m_s)B_0$ with $\hat{m} = \frac{1}{2}(m_u + m_d)$, one can easily translate this into a relation between the critical values of m_K and m_π: $m_K^2 = m_K^2\big|_{TCP} + \frac{m_\pi^2}{2} - \alpha m_\pi^{4/5}$. Due to the failure of our parametrization at very high values of m_K, and near the $m_\pi = 0$ axis we use this formula to extrapolate the upper edge of the phase boundary to the m_K-axis. Using large N_c ChPT theory we obtain $m_K^{TCP} = 1718$ MeV, while using the Veneziano formula (27) we get $m_K^{TCP} = 1838$ MeV. Both fits are of very good quality suggesting the radius of the scaling region to be $\Delta m_\pi^c \approx 40$ MeV. In terms of the strange quark mass our estimate corresponds to $m_s^{TCP} = 13 - 15 \times m_s$. This result can be compared to the recent lattice result of [29], where it was estimated that $m_s^{tric} \approx 3m_s$. In case of [29] the piece of the phase boundary used in the extrapolation to m_s^{TCP} was much closer to the physical point and the location of the TCP was estimated using points with $m_s \leq m_s^{phys}$. The lattice estimate for the location of TCP would improve if points could be simulated closer to the scaling region.

In the present treatment the critical pseudoscalar mass for degenerate quarks was obtained in the range $m_\pi^c \in (90, 130)$ MeV. The spread is the result of the renormalization scale dependence. This range of m_π^c is significantly above the one previously obtained in [14] using a tree-level parametrization, which eventually led to $m_\pi^c \in (20, 60)$ MeV. It is interesting to note, that the boundary lies to the right from the fitted curves which describe the scaling behavior near TCP.
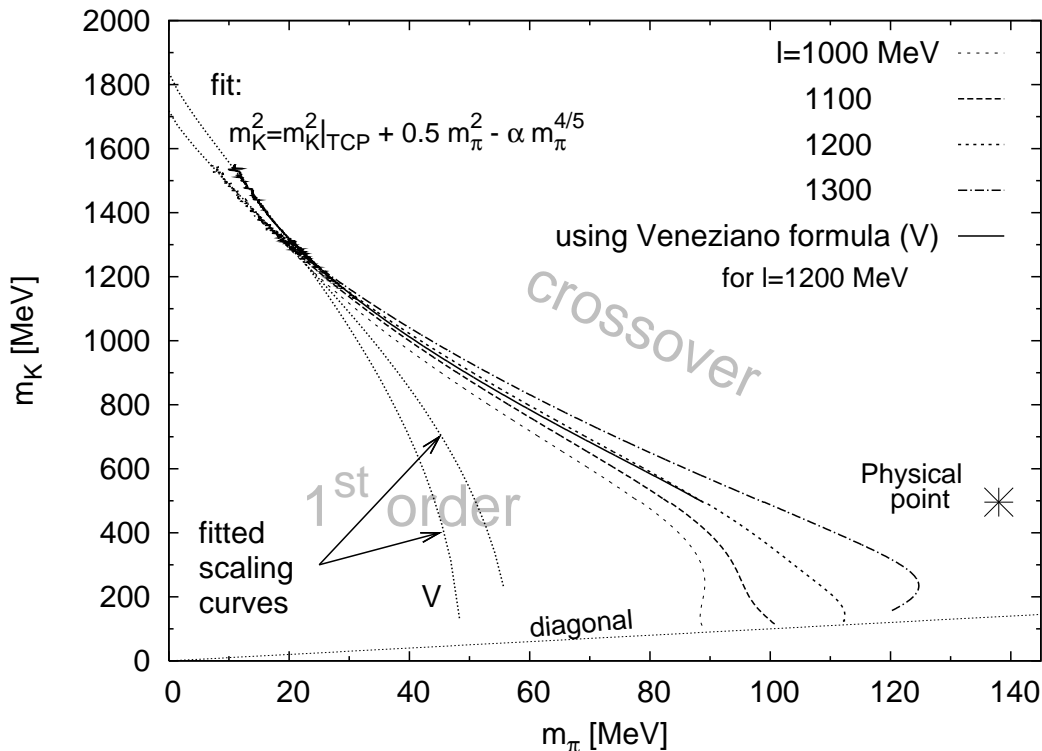
FIG. 7: Phase boundary of LσM obtained using a one-loop parametrization at $T = 0$ and the formulas of large N_c ChPT for continuation on the $m_\pi - m_K$–plane. For large values of m_K we have also used the Veneziano formula for m_η cf. II B.

---

[1] It can be seen after some straightforward calculation, that as the kaon mass increases, the relative weight of the terms containing $\log(l)$ are becoming negligible in the equations used for parametrization as well as in those used for thermodynamic calculations.

V.   CONCLUSION

In this paper we have studied the phase boundary of the linear sigma model in the $m_\pi - m_K$ plane. We have managed to find in a resummed perturbation theory a set of renormalized equations based on which complete one-loop parametrization of the model is possible not only at the physical point, but in a large region of the mass-plane too. We allowed for the variation of the parameters with m_π and m_K when moving away from the physical point, and used formulas of the ChPT for the continuation of certain physical quantities into the mass–plane.

As a result of the one-loop solution of the model we were able to estimate the location of the tricritical point on the $m_\pi = 0$ axis of the mass plane at a rather high value of the kaon mass. We have shown evidence of the existence of a scaling region around it. These were not observed previously in the quasi-particle approximations to the model. For the same values of m_K the phase boundary line lies at higher values of pion masses than in the case of the tree-level parametrization of the model, and without the inclusion of the vacuum fluctuations. For degenerate pseudoscalar masses the phase boundary was obtained in the range $m_\pi^c \in (90, 130)$ MeV.

We have discussed also the limitation of the optimized perturbation theory, related to the fact that one looks for real solutions of the gap-equation for the resummed mass in temperature ranges where the self-energies develop imaginary parts too. It would be interesting to study the phase boundary using a self-consistent approximation based on the exact propagator, like the 2PI approximation.

Acknowledgement

APPENDIX A: CONNECTION BETWEEN $(0-8)$ AND $(X-Y)$ BASIS

From the $x - y$ basis used in section II one can obtain, with the help of an orthogonal transformation, the mixed scalar-, pseudoscalar and the external fields in the conventional $(0 - 8)$ basis as:

$$\begin{pmatrix} \sigma_0 \\ \sigma_8 \end{pmatrix} := O \begin{pmatrix} \sigma_x \\ \sigma_y \end{pmatrix}, \begin{pmatrix} \pi_0 \\ \pi_8 \end{pmatrix} := O \begin{pmatrix} \pi_x \\ \pi_y \end{pmatrix}, \qquad \begin{pmatrix} \epsilon_0 \\ \epsilon_8 \end{pmatrix} := O \begin{pmatrix} \epsilon_x \\ \epsilon_y \end{pmatrix}, \text{ where } O := \frac{1}{\sqrt{3}} \begin{pmatrix} \sqrt{2} & 1 \\ 1 & -\sqrt{2} \end{pmatrix}. \tag{A1}$$

The transformation of the mass matrices, and the mass eigenvalues are

$$\begin{pmatrix} m_{\eta_{00}}^2 & m_{\eta_{08}}^2 \\ m_{\eta_{08}}^2 & m_{\eta_{88}}^2 \end{pmatrix} = O \begin{pmatrix} m_{\eta_{xx}}^2 & m_{\eta_{xy}}^2 \\ m_{\eta_{xy}}^2 & m_{\eta_{yy}}^2 \end{pmatrix} O, \quad \text{and} \quad m_{\eta',\eta}^2 = \frac{m_{\eta_{xx}}^2 + m_{\eta_{yy}}^2 \pm \sqrt{(m_{\eta_{xx}}^2 - m_{\eta_{yy}}^2)^2 + 4m_{\eta_{xy}}^4}}{2}. \tag{A2}$$

Similar expressions also hold for the scalar fields.

APPENDIX B: WARD IDENTITIES

From (8) and (13), the inverse pion and kaon propagators at zero external momenta are

$$-iZ_\pi^{-1} D_\pi^{-1}(p=0) = m_\pi^2 + \Sigma_\pi(p=0) + \Delta m^2 \tag{B1}$$
$$-iZ_K^{-1} D_K^{-1}(p=0) = m_K^2 + \Sigma_K(p=0) + \Delta m^2, \tag{B2}$$

where the finite counterterms of OPT are now explicitly indicated. Comparing the expressions of tree-level masses (Table I) with the tree-level part of the equations of state (28), (29), one can obtain the corresponding tree-level Ward identities $\epsilon_x = m_\pi^2 x$ and $\epsilon_y = m_K^2(\sqrt{2}/2 x + y) - m_\pi^2 \sqrt{2}/2 x$. The diagrams for the self-energies are shown in Fig. 1. They include both tadpole and bubble diagrams, and the latter ones can be decomposed for non-equal propagator masses and zero external momenta into the difference of two tadpoles:

$$\cdots \bigcirc \cdots = \frac{1}{m_1^2 - m_2^2} \cdot \left[\bigcirc - \bigcirc \right]. \tag{B3}$$

Therefore, the pseudoscalar self energies at $p = 0$ can be represented as a linear combination of tadpole contributions whose weights are complicated expressions of the tree-level masses and the corresponding four- and three-point couplings

(see [11]). In the case of pion and kaon these weights simplify to

$$\Sigma_\pi(p=0) \;=\; \frac{\sum J_i t_i^x I(m_i,l) + x\Delta m^2}{x}\,, \tag{B4}$$

$$\Sigma_K(p=0) \;=\; \frac{\sum J_i(t_i^x + \sqrt{2}t_i^y)I(m_i,l) + (x+\sqrt{2}y)\Delta m^2}{x+\sqrt{2}y}\,, \tag{B5}$$

where $I(m_i,l)$ is the $T=0$ tadpole integral and the sum goes over all mass eigenstate meson fields with isospin multiplicity J_i. Substituting these and the corresponding tree-level Ward identities into the expressions (8), (13), one can obtain the equations of state (28) and (29), which determine the external fields at zero temperature in the parametrization process. The relations (22) and (23) are also valid at finite temperature and ensure the fulfillment of Goldstone's theorem at one-loop order.

APPENDIX C: PCAC RELATIONS

The one-loop order PCAC relations for the pion and kaon are given in [11] by

$$f_\pi M_\pi^2 = \sqrt{Z_\pi}\epsilon_x\,, \qquad f_K M_K^2 = \frac{\sqrt{Z_K}\epsilon_y}{\sqrt{2}} + \sqrt{Z_\pi}\epsilon_x\,. \tag{C1}$$

With the help of (22), (23) the external fields can be eliminated and one can obtain the expressions (20), (21), which appear renormalization scale-dependent. However, one can rearrange the pion self-energies appearing in (20) as follows:

$$f_\pi = \frac{m_\pi^2 + \Sigma_\pi(p=0,l)}{M_\pi^2}Z_\pi^{-\frac{1}{2}} \;=\; \frac{m_\pi^2 + \Sigma_\pi(p^2=M_\pi^2,l) + (\Sigma_\pi(p=0,l) - \Sigma_\pi(p^2=M_\pi^2,l))}{M_\pi^2}Z_\pi^{-\frac{1}{2}}$$

$$= \left(1 - \frac{\tilde{\Sigma}_\pi(p^2=M_\pi^2)}{M_\pi^2}\right)Z_\pi^{-\frac{1}{2}}. \tag{C2}$$

In the last step above we used the fact, that $m_\pi^2 + \Sigma_\pi(p^2=M_\pi^2)$ is just the definition of the pole mass M_π^2. The p-dependent part of the self energy, $\tilde{\Sigma}$, like the wave function renormalization constant, does not depend on the renormalization scale and in consequence (C2) is actually scale-independent. The PCAC equation for the kaon can be analyzed in a similar way.

---

[1] D. Röder, J. Ruppert and D. H. Rischke, Phys. Rev. D **68**, 016003 (2003) [nucl-th/0301085].
[2] P. Costa, M. C. Ruivo, C. A de Sousa and Yu. L. Kalinovsky, Phys. Rev. D **71**, 116002 (2005) [hep-ph/0503258].
[3] S. Michalski, [hep-ph/0601255].
[4] A. Barducci, R. Casalbuoni, G. Pettini, L. Ravagli, Phys. Rev. D **69**, 096004 (2004) [hep-ph/0402104].
[5] H. J. Warringa, D. Boer, J. O. Andersen Phys. Rev. D **72**, 014015 (2005) [hep-ph/0504177].
[6] R. D. Pisarski and F. Wilczek, Phys. Rev. D **29**, 334 (1984).
[7] Z. Fodor, S.D. Katz, JHEP 0404 (2004) 050 [hep-lat/0402006].
[8] F. Karsch, E. Laermann, Ch. Schmidt, Phys. Lett. **B520**, 41 (2001) [hep-lat/0107020].
[9] N. H. Christ, X. Liao, Nucl. Phys. Proc. Suppl. **119**, 514 (2003).
[10] F. Karsch, C. R. Allton, S. Ejiri, S. J. Hands, O. Kaczmarek, E. Laermann and C. Schmidt, Nucl. Phys. Proc. Suppl. **129-130**, 614 (2004) [hep-lat/0309116].
[11] L.-H. Chan and R. W. Haymaker, Phys. Rev. D **7**, 402 (1973) [nucl-th/9901049].
[12] N. A. Törnqvist, Eur. Phys. J C **11**, 359 (1999) [hep-ph/9905282].
[13] J.T. Lenaghan, D. H. Rischke and J. Schaffner-Bielich, Phys. Rev. D **62**, 085008 (2000) [nucl-th/0004006].
[14] T. Herpay, A. Patkós, Zs. Szép, P. Szépfalusy Phys. Rev. D **71**, 125017 (2005) [hep-ph/0504167].
[15] A. Jakovác, A. Patkós, Zs. Szép, P. Szépfalusy Phys. Lett. B **582**, 179 (2004) [hep-ph/0312088].
[16] S. Chiku and T. Hatsuda, Phys. Rev. D **58**, 076001 (1998) [hep-ph/9803226].
[17] J. M. Cornwall, R. Jackiw, and E. Tomboulis, Phys. Rev. D **10**, 2428 (1974).
[18] J. T. Lenaghan, D. H. Rischke, J. Phys. **G26**, 431 (2000) [nucl-th/9901049].
[19] H. Hees, J. Knoll, Phys. Rev. D65, 025010 (2002) [hep-ph/0107200].
[20] J.-P. Blaizot, E. Iancu, U. Reinosa Phys. Lett. **B 568**, 160 (2003) [hep-ph/0301201]; Nucl. Phys. **A 736**, 149 (2004) [hep-ph/0312085].
[21] J. Berges, Sz. Borsányi, U. Reinosa, J. Serreau, Annals Phys. **320**, 344 (2005) [hep-ph/0503240].
[22] Yu. B. Ivanov, F. Riek, H. van Hees, J. Knoll Phys. Rev. D **72** (2005) 036008 [hep-ph/0506157].
[23] A. Jakovác and Zs. Szép, Phys. Rev. D **71**, 105001 (2005) [hep-ph/0405226].
[24] A. Patkós, Zs. Szép, P. Szépfalusy Phys. Rev. D 66 (2002) 116004 [hep-ph/0206040].
[25] J. Gasser, H. Leutwyler, Nucl. Phys. **B250**, 465 (1985).
[26] P. Herrera-Siklódy, J. I. Latorre, P. Pascual, J. Taron, Phys. Lett. B **419**, 326 (1998) [hep-ph/9710268].
[27] G. Veneziano, Nucl. Phys. **B159**, 213 (1979).
[28] Y. Hatta, T. Ikeda, Phys. Rev. D **67**, 014028 (2003) [hep-ph/0210284].
[29] O. Philipsen, PoS LAT2005 (2005) 016 [hep-lat/0510077].